# Transport and diffusion in nanopores

***Course project : Transport Phenomena I***

Christoph Csoklich, Sthavishtha Bhopalam Rajakumar, Tess Colijn
ETH Zürich, Switzerland

December 21, 2018

## 1 Introduction

In the absence of boundaries, a particle obeys Brownian motion. This random motion can be described with changes in direction and speed, which occur due to the collisions with other particles. For an unbounded particle, the diffusion coefficient is proportional to temperature and inversely proportional to the friction coefficient. In microporous materials (having pore diameters less than 2 nm) such as zeolites, the pores form an array that can act as sites of confinement for particles or molecules. Diffusion within these confined channels is directed by an external potential and can be described with Langevin dynamics in the over-damped limit with reflecting boundary conditions at the impenetrable channel walls, given as follows [1]:

$$\eta \dot{\boldsymbol{r}}(\tilde{\boldsymbol{t}}) \;=\; -\boldsymbol{F} \;+\; \sqrt{\eta k_B T}\boldsymbol{\xi}(\tilde{t}) \tag{1}$$

where $\eta$ represents the friction coefficient, $k_B$ the Boltzmann constant, $\tilde{t}$ the non-dimensionalized time, T the temperature, r the position vector of the particle and $\xi(\tilde{t})$ the random variable. This random variable represents the Gaussian white noise modeling of thermal fluctuations, following the Sutherland-Einstein fluctuation-dissipation relation : $\langle \xi(\tilde{t}) \rangle = 0$ and $\langle \xi_i(\tilde{t}) \xi_j(\tilde{t}^{'}) \rangle = 2\delta_{ij}\delta(\tilde{t} - \tilde{t}^{'})$, for $i, j = 1, 2$.

In a purely energetic system, entropy increases as the temperature increases. However, diffusion through nanopores can be considered as an entropic behavior. The bottlenecks between the nanopores form entropic potential barriers which cause an increase in entropy if the particles move from one pore to another. This entropic nature change depends on the ratio between the width of the pores and the width of the bottlenecks. Closer the ratio to unity implies less entropic diffusion behavior as both the widths will be equal. This entropic behavior causes spatial variation of the entropy affecting the heat and mass transport. As the bottlenecks get wider, more will be the space for the particle to remain in the bottleneck, thus restricting its motion. In other words, an increase in the bottleneck size increases the number of accessible states. A flat channel without any obstacles in the presence/absence of an external force (bias) will not vary the diffusion coefficient. However, narrow channels with obstacles (due to the varying complex shape of the boundaries) in the direction of propagation, affect the transport properties (including the diffusion coefficient) due to the coupling between the transverse and longitudinal directions of motion [2]. This leads to a spatially varying diffusion coefficient [3]. In such cases of entropic barriers, the particle motion gets characterized by an effective diffusion coefficient, which is smaller than the particle diffusion coefficient. As the channel gets narrower, the effective diffusion coefficient decreases [4]. Additionally, in a non-entropic system, temperature and force are independent and treated as such. However, in an entropic behavior, the applied force and temperature can be coupled. Thus, a decrease in temperature will lead to an increase in (dimensionless) force, thus increasing the nonlinear mobility and the likeliness of a transition. This implies faster mass transfer with a large increase in the entropy.

## 2 Brownian dynamics simulations

The overdamped Langevin Eqn. 1 has been numerically simulated using the Brownian dynamics approach, in the current section. The following non-dimensional equations have been followed :

$$x(t+1) \;=\; x(t) \;+\; F_x \Delta t \;+\; \sqrt{D\Delta t}\xi_1 \tag{2}$$

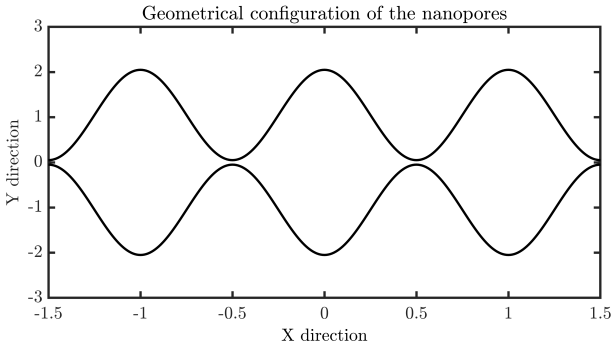


Figure 1: Geometrical configuration of the nanopores

$$y(t+1) \;=\; y(t) \;+\; \sqrt{D\Delta t}\xi_2 \tag{3}$$

where $\xi_1$ and $\xi_2$ are random numbers extracted from a normal distribution for each time step, having zero mean and unity variance. In the above equations, the force term represents a constant (drift) velocity taken to be along $x$ direction. The input parameters in the Brownian dynamics simulation include the number of trajectories (NTRA), the total number of time steps for which diffusion is simulated (NTIME) and the time step (DT). In the current work, three continuous nanopores of the form $y(x) = \cos(2\pi x) + 1.05$ are considered. At the beginning of the simulation, all the Brownian particles are placed at the center of the domain ($(0,0)$, as per Fig. 1), for simplicity. Thus, the probability distribution would take the form of a delta distribution.

The left and right end boundaries of the domain are considered to be absorbing in the current case, meaning that the particles leave the domain on reaching these boundaries. Additionally, the top and bottom nanopore boundaries are taken to be reflecting, such that the particles leaving these boundaries are replaced by its respective position in the previous time step [2].

The effective diffusion coefficients $D_{eff}$ along the $x$ direction have been computed as follows [2]:

$$D_{eff} \;=\; \frac{\langle x_i^2(t)\rangle - \langle x_i(t)\rangle^2}{t} \tag{4}$$

For the aforementioned parameters, the diffusion coefficients have been computed from the slope of the graph in Fig. 2. To be consistent with the absorbing boundary conditions at the left and right boundaries, the variance of the Brownian particles' positions escaping these boundaries are not taken into account while calculating the effective diffusion coefficient. As seen in Fig. 2, $D_{eff,y} = 0.6119$ and $D_{eff,x} = 0.1375$ have been obtained. The large value of $D_{eff,y}$ in comparison to $D_{eff,x}$ verifies the consistency of the simulation for a faster equilibration in the transverse direction than in the longitudinal direction. Thus, this confirms the phenomenological idea of entropic diffusion in nanopores.

Burada et al obtained a $D_{eff,x}$ of approximately 0.5. This one-dimensional result was obtained using periodic nanopores and the additional assumption that the degree of freedom in the y-direction can be eliminated due to a faster equilibration [1].

To study the effect of force on the Brownian particles, a constant non-dimensional force of unity has been assumed along the $x$ direction, as per Eqn. 2. As seen in Fig. 3, a force causes the particles to shift in its direction, causing the probability distribution to yield another gaussian peak in the adjacent pore.

## 3 Numerical solution of the Fokker-Planck equation

The Fokker-Planck equations for the system can be given by :

$$\frac{\partial P(\mathbf{x},t)}{\partial t} \;=\; -\nabla\cdot\mathbf{J}(\mathbf{x},t) \tag{5}$$

$$\mathbf{J}(\mathbf{x},t) \;=\; F_x P(\mathbf{x},t) \;-\; \frac{1}{2}\nabla(D(\mathbf{x})(P(\mathbf{x},t)) \tag{6}$$

Where $\mathbf{J}(\mathbf{x},t)$ represents the probability current.

The above Eqns. 5 and 6 are solved using a finite difference method (FDM). The effective diffusion coefficients calculated from the Brownian dynamics simulation in the absence of force ($D_{eff,y}$ of 0.6119

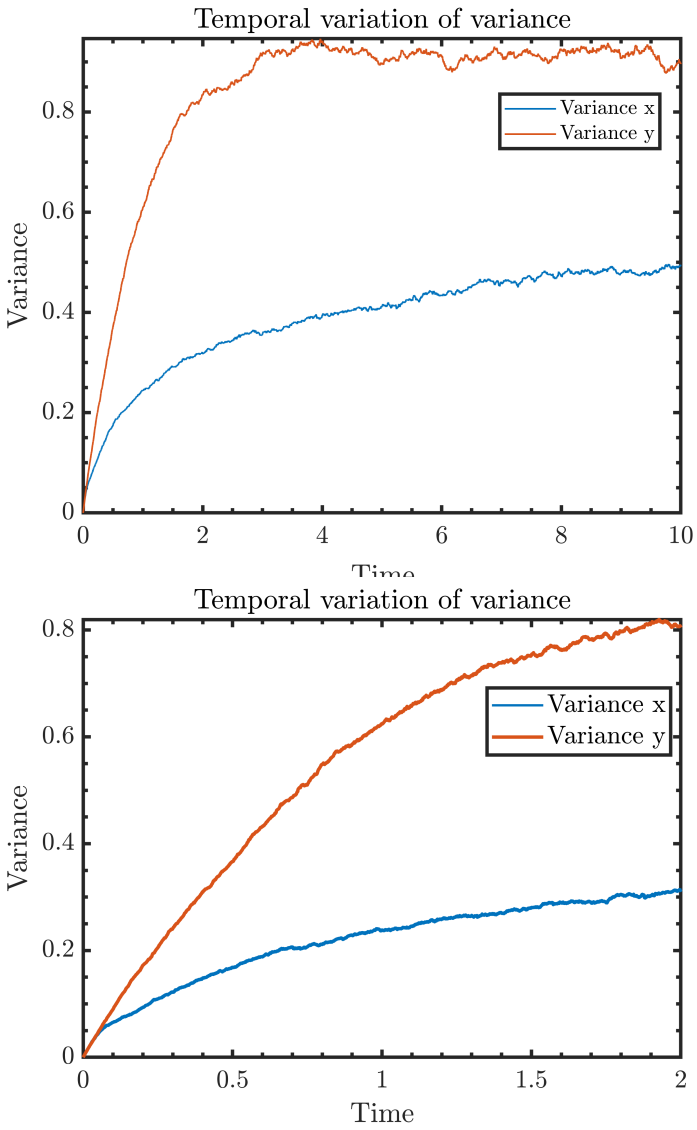


Figure 2: Temporal variation of variance; The variance reaches a plateau at large time steps (above). The slope is extracted from the linear region of this plot (below) to compute the diffusion coefficients.

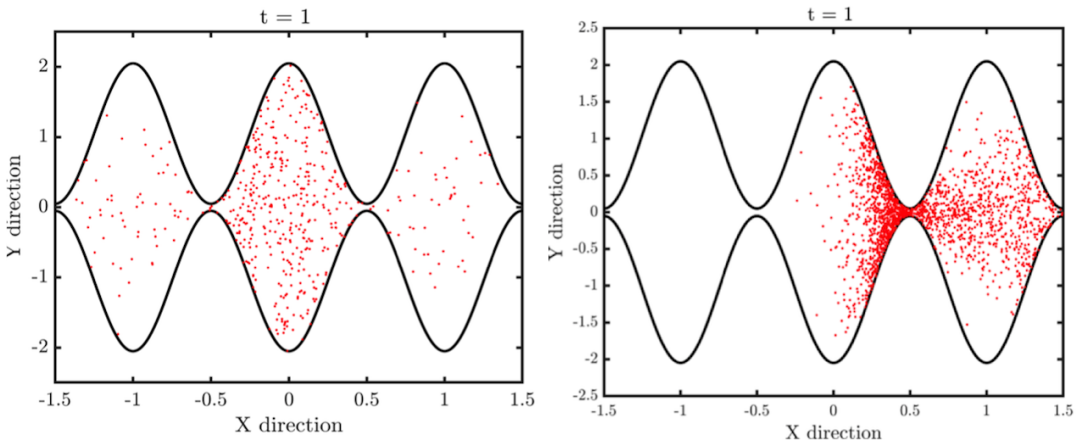


(a) $Force = 0$ (b) $Force = 1$

Figure 3: Positions of the particles in the a) absence of force and b) presence of force

and a $D_{eff,x}$ of 0.1374) are used for numerically solving these equations. An explicit first order with time and second-order central differencing scheme (CDS) with space are used as follows for discretization:

$$\frac{\partial P(\mathbf{x},t)}{\partial t} = \frac{P_{i,j}^{t+1} + P_{i,j}^{t}}{\Delta t} \tag{7}$$

$$F_x P(\mathbf{x},t) = F_x\left(\frac{P_{i+1,j}^{t} + P_{i-1,j}^{t}}{2\Delta x}\right) \tag{8}$$

$$\nabla(D(\mathbf{x})(P(\mathbf{x},t)) = D_{eff,x}\left(\frac{P_{i+1,j}^{t} - 2P_{i,j}^{t} + P_{i-1,j}^{t}}{(\Delta x)^2}\right) \tag{9}$$

To be consistent with the absorbing boundary conditions at the left and right boundaries used in the Brownian dynamics simulations, $P = 0$ has been chosen at every iterating time step. Additionally, the top and bottom boundaries are assumed as no flux boundaries implemented into the simulation with the equation:

$$\mathbf{J}(\mathbf{x},t)\cdot\mathbf{n} = 0 \tag{10}$$

Where $\mathbf{n}$ represents the normal to the wall, with the nanopores' shape approximated with a staircase representation. For the same initial delta probability distribution used earlier, the numerical solution of the Fokker-Planck equation gives a probability distribution of a Gaussian form, as seen in Fig. 4 at $t = 1$, in the absence of force. Good agreement between these curves is observed, which validates the approach used. The slight deviation can be noticed particularly at the Gaussian peaks, which could be improved on using a grid independent mesh.

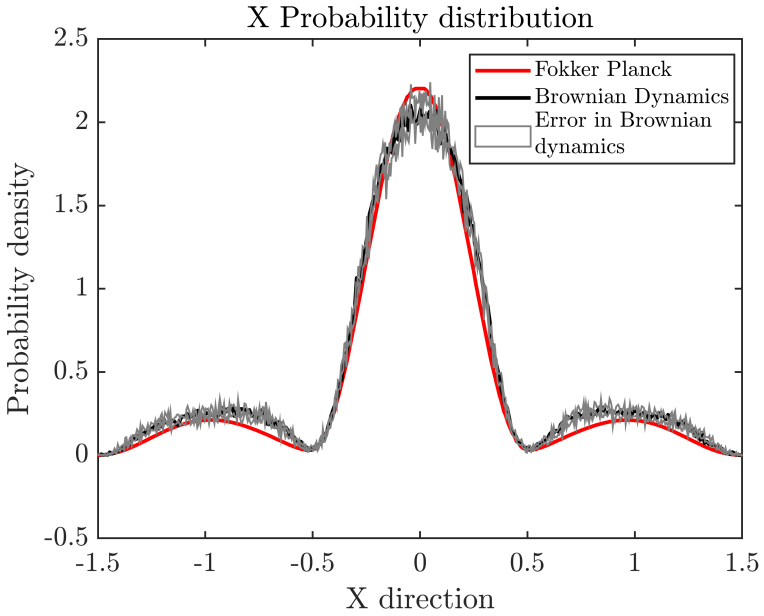


Figure 4: Normalized probability distributions at $t = 1$ obtained with brownian dynamics and Fokker-Planck approaches

## 4 Active Brownian dynamics (extension task)

In the case of active Brownian dynamics, the particles are assumed to propel in random directions (eg. bacteria). In that case, an extra Langevin equation conserving the angular velocity has to be numerically solved. Additionally, the Brownian particles will move along this angular orientation with a propulsion velocity. Accordingly, the equations are [5]:

$$x(t+1) = x(t) + F_x\Delta t + v\Delta t\cos\theta(t) + \sqrt{D\Delta t}\xi_1 \tag{11}$$

$$y(t+1) \;=\; y(t) \;+\; v\Delta t \sin\theta(t) + \;\sqrt{D\Delta t}\xi_2 \tag{12}$$

$$\theta(t+1) \;=\; \theta(t) \;+\; \sqrt{D\Delta t}\xi_3 \tag{13}$$

In the current study, $F_x$ and $v$ have been taken to be zero and unity respectively. The positions of the particles are illustrated in Fig. 5, while the variance is shown in Fig. 6. Enhanced effective diffusion is observed leading to $D_x = 0.14$ and $D_y = 0.64$, which are slightly higher compared to the passive particles. This is because of the fact that the variance is a function of the propulsion speed and angular position [5]. Additionally, the rotational diffusion coefficient $D_{rotation} = 1.09$, is the same as the particle diffusion coefficient (unity) due to the fact that the angular motion of the particles is not confined.

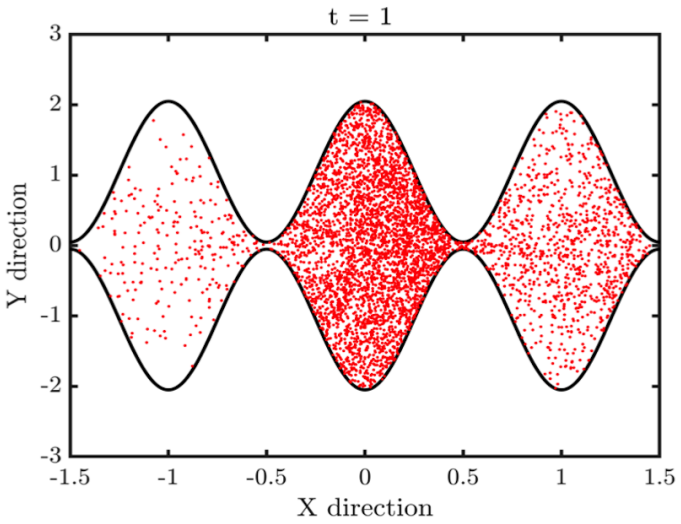


Figure 5: Positions of the active brownian particles

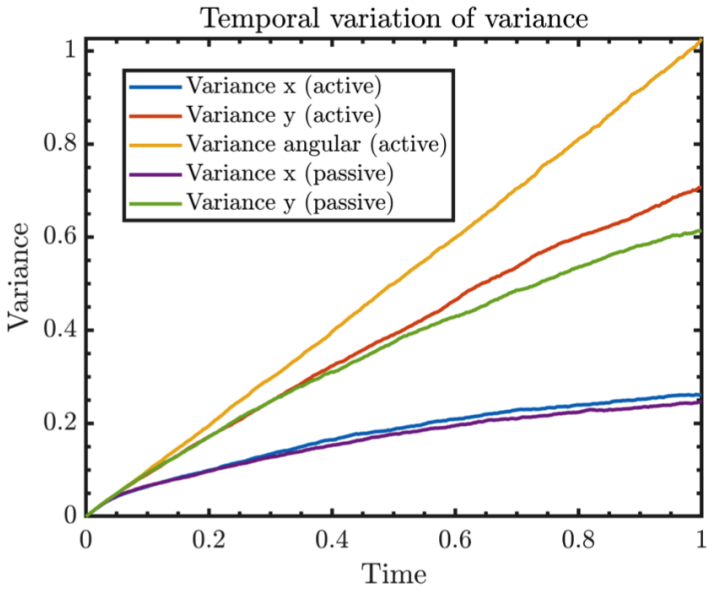


Figure 6: Temporal variation of variance in the case of active brownian particles

## 5 Acknowledgements

The authors thank Meisam Pourali for his help and guidance during the due course of this project.

# References

[1] P Sekhar Burada, Gerhard Schmid, and Peter Hänggi. Entropic transport: a test bed for the fick–jacobs approximation. *Philosophical Transactions of the Royal Society of London A: Mathematical, Physical and Engineering Sciences*, 367(1901):3157–3171, 2009.

[2] P Sekhar Burada. *Entropic transport in confined media*. PhD thesis, Universität Augsburg, 2008.

[3] Robert Zwanzig. Diffusion past an entropy barrier. *The Journal of Physical Chemistry*, 96(10):3926–3930, 1992.

[4] Marcio-Vinicio Vazquez, Alexander M. Berezhkovskii, and Leonardo Dagdug. Diffusion in linear porous media with periodic entropy barrier: A tube formed by contacing sphreres. *The Journal of Chemical Physics*, 129(4), 2008.

[5] Giorgio Volpe, Sylvain Gigan, and Giovanni Volpe. Simulation of the active brownian motion of a microswimmer. *American Journal of Physics*, 82(7):659–664, 2014.